

# Using Powder Metallurgy and Oxide Reduction to Produce Eco-Friendly Bulk Nanoporous Nickel

Mark A. Atwater<sup>1,\*</sup>, Sean Corcoran<sup>2</sup>

<sup>1</sup> Mechanical Engineering, Liberty University, Lynchburg, VA, USA

<sup>2</sup> Materials Science and Engineering, Virginia Tech, Blacksburg, Virginia 24061, USA

\*Corresponding Author: matwater1@liberty.edu

## Abstract

A low cost and scalable powder-based method for producing nanoporous Ni is demonstrated, and the only processing byproduct is water vapor. This is achieved by creating a metal-matrix composite of Ni and NiO that is then reduced under dilute hydrogen to create pure Ni with nanocrystalline structure and nanoscale porosity. The technique is demonstrated in loose powder and in thin and bulk compacts with centimeter dimensions. These compacts can withstand extensive deformation without disintegrating, performing similarly to wrought Ni in specific strength. The unique processing strategy and resulting material can be readily extended to other metals and alloys.

Keywords: nanoporous; nickel; nanocomposite; mechanical milling; foaming

## 1 Introduction

Nanoporous (np) metals and alloys are candidates for functional applications due to their high surface area, and the most studied technique for creating them is dealloying [1, 2]. Dealloying selectively removes a more chemically active element from a precursor alloy and creates a bicontinuous pore structure with nanoscale ligaments and voids. The detailed microstructural study of np materials was not initiated until the mid-20<sup>th</sup> century, even though dealloying was identified earlier [2]. The mechanisms of pore formation were established even more recently [3, 4], and the understanding and diversity of the structures has grown rapidly since then [2]. The technique of dealloying was traditionally applied via direct chemical corrosion, but the method has since been extended to include liquid, solid, and vapor phase dealloying.

It is important to note that all dealloying methods employ some chemical aspect to the process, but “free” corrosion and electrochemical corrosion methods are most closely linked to the metal-etchant chemistry. In a binary alloy, the dealloying process selectively leaches the more active of the two elements when it is present above the parting limit (minimum concentration for pore formation) rather than passivating the surface. This results in the formation of islands of the more noble element, which allows the continued etching of the material and eventually a bicontinuous structure [3, 4]. When using *electrochemical* dealloying (adding an electrical potential in addition to the chemical activity), the final morphology can be controlled [5], and even the more noble element can be preferentially etched [6]. Chemical dealloying can also be applied to ternary alloys [7-10] and amorphous alloys (metallic glasses) [11-13]. These multi-element materials have greater microstructural stability [9, 14, 15], which is important to reliably applying them.

This article has been accepted for publication and undergone full peer review but has not been through the copyediting, typesetting, pagination and proofreading process, which may lead to differences between this version and the [Version of Record](https://onlinelibrary.wiley.com/doi/10.1002/adem.202201629). Please cite this article as doi: [10.1002/adem.202201629](https://onlinelibrary.wiley.com/doi/10.1002/adem.202201629)

This article is protected by copyright. All rights reserved

To broaden the range of np metals beyond the practical limits of chemical dealloying, a new method, liquid metal dealloying (LMD), was introduced in which an element is removed by an alloy exchange with another, more “preferred” metal. The precursor alloy is placed in a molten metal bath that has a larger negative heat of mixing with one of the precursor elements. The dealloying process will continue until the bath is saturated with that element [16, 17]. For example, Wada et al. describe the dealloying of Cu from a Ti-Cu alloy in a Mg melt where Cu atoms preferentially mix with the Mg [18]. This technique allows non-noble metals to be dealloyed (e.g., [19–22]), but it creates an interpenetrating two-phase solid that must still be chemically etched to produce the final porosity, although more recent work demonstrates liquid metal expulsion at the conclusion of LMD is possible [23]. A variation on this, solid metal dealloying (SMD), is analogous to LMD, but the process is dependent on a solid state diffusion couple, results in slower kinetics, and is suitable for conformations such as thin films [24, 25]. Once again, the final alloy must be etched to create porosity from the phase-separated solid. In practice, these methods create two-phase mixtures for chemical etching and are therefore more complex than direct chemical methods to create np metals.

Another recent development in np metal production is vapor phase dealloying (VPD). In this method, the varying vapor pressures of elements are utilized to selectively remove one of them by thermal processing. It is clearly demonstrated in a report by Lu et al. [26] where Zn is “etched” from a Co-Zn alloy under high vacuum and elevated temperature to produce np Co. This technique is touted as being environmentally friendly, as the vaporized Zn can be recovered. A somewhat related vapor-phase process involves the treatment of a Au-Ag alloy to cause rapid diffusion of Ag to the surface using ozone thereby creating interfacial porosity that is completed by treatment in methanol and oxygen [27]. Pulsed laser energy can be used to selectively sublime elements, like Zn from a Cu-Zn alloy, and produce nanoscale pores in the surface of a component (depth of ~50  $\mu\text{m}$ ) [28, 29]. The latter two techniques are surface dealloying processes only, and this type of treatment has actually been applied since antiquity in “depletion gilding” [4]. Commercially purchased brass powders have also been thermally dealloyed under vacuum (removal of zinc) to create *microporous* Cu [30, 31].

Dealloying is not the only option for creating nanoporous structures, although it is the most widely used and developed. In brief, other related methods include reduction induced decomposition, which has been demonstrated using AgCl [32], such that Ag is left behind and Cl<sup>-</sup> ions are produced in a reaction with aqueous NaBH<sub>4</sub> and a bicontinuous pore structure is created. This removes the need to create a precursor alloy, though the compound must still be created. Another related process is metal-induced crystallization (MIC), which has been demonstrated in sputtered Au-Ge bilayers that result in a two-phase Au-Ge composite upon heating [33]. The Ge is then etched using H<sub>2</sub>O<sub>2</sub> to create nanoscale porosity.

Methods significantly different from dealloying include dynamic hydrogen bubble templating (DBHT) [34], which can be considered a poorly conducted electrochemical deposition process, as porosity in these deposits is not typically desirable. The structure of np electrodeposited films is characterized by dendritic or other highly textured features (also referred to as a ramified structure) that increase the overall surface area of the material (often by hundreds of times [35]). Tappan et al. [36] review a collection of processes that are more chemistry intensive, such that exothermic reactions, sol-gel processing, foaming agents, etc. are involved in creating the final three-dimensional np *networks*. As noted there, combustion synthesis is perhaps the most promising, and it uses the kinetically self-controlled decomposition of a metal-bistetrazolamine (MBTA) compound that creates a type of metallic aerogel. Likewise, network templating/scaffolding methods [37, 38] can be used to create networks of nanoscale particles and pores. The processing techniques include colloidal nanoparticle methods, physical vapor deposition, and natural templates (e.g., protein nanofibrils). In general, these methods are outside the scope of this work and less developed for np metals than dealloying methods.

The production of np metals and alloys is a highly active area of research and development, not only in the frequency of publication, but also in the development of new methods. Although quite successful, dealloying has drawbacks. As noted by Zhang et al. [33], challenges include residual material from the sacrificial phase, complicated processing to produce the precursor alloy, hazardous chemicals required for corrosion, and the tendency to form microcracks. While the significance of each depends on the alloy system, processing strategy, and application, continued advancement on simplicity, scalability, and environmental impact is needed.

To that end, a process has been developed to produce np metals and alloys that addresses the following challenges: (1) simple, scalable production of precursor materials, (2) no hazardous chemicals, byproducts, or residues, (3) bulk geometries readily made, and (4) mechanically robust structure. In addition, the method presented only requires modest process temperatures and can be implemented at scale using current manufacturing technology. The strategy employs the vapor-phase reduction of oxide particles dispersed within a metallic matrix. This process is a unique adaptation of the Additive Expansion by the Reduction of Oxides (AERO) method, which has been successfully implemented in Cu [39], Ni [40], Ag [41], and alloys of them. The current embodiment is distinctly different from “traditional” AERO embodiments in that the oxide phase is the dominant component, requires lower processing temperature, and results in a bicontinuous nanoscale pore structure.

## 2 Experimental Methods

### 2.1 Material Preparation

To prepare the precursor powders, Ni (Sigma-Aldrich, p/n 266981, 99.7%, < 50  $\mu\text{m}$ ) and NiO (US Research Nanomaterials, p/n US3355, 99.5%, 15–35 nm) were ball milled in a SPEX 8000D mixer/mill at room temperature for 1 hr in a 440C stainless steel vial with 440C stainless steel ball bearings using 17 bearings with diameter of 7.94 mm and 16 bearings with 6.35 mm diameter (10:1 ball-to-powder mass ratio). Vials and bearings were cleaned with ethanol, and all materials were stored, loaded, and milled under Ar (less than 1 ppm  $\text{O}_2$  and  $\text{H}_2\text{O}$  measured and maintained within Inert Corp. glove box). Three sample types were analyzed: 90 mol% NiO (10% Ni) to create a metal matrix composite (MMC) denoted as Ni90NiO, As-Received NiO nanopowder (AR-NiO), and pure NiO nanopowder milled identically to Ni90NiO (M-NiO). AR-NiO and M-NiO were used as control samples, as was pure Ni powder (unmilled) for reduction onset purposes. These powders were then reduced in a 5%  $\text{H}_2$  (balance Ar) atmosphere flowing at 400 sccm within a 50 mm diameter tube furnace (Across International, STF-1200) while recording the moisture content in the exhaust gas stream using an Omega HX-200 humidity meter. The reduction onset temperature of the oxide was determined by inserting the sample boat into the furnace before starting the furnace at a 5  $^\circ\text{C}/\text{min}$  ramp to 600  $^\circ\text{C}$ . The isothermal reduction characteristics were determined by pre-heating the furnace to the desired temperature and then inserting the sample into the furnace. The starting dewpoint was -60.0  $^\circ\text{C}$  ( $\sim 10.5$  ppm  $\text{H}_2\text{O}$ ), which is the minimum measurable with this sensor.

To investigate the production of bulk components and their properties, uniaxial pressing at 1 GPa and 400  $^\circ\text{C}$  under Ar was performed to create disks and pellets. A 12 mm tungsten carbide die was used in conjunction with a custom pressing chamber and a 40-ton Carver AutoPellet (model 4387.1NE) to preheat the material and die for 30 min then apply the desired pressure and maintain it for a period of 10 min. Thin disks ( $\sim 200$   $\mu\text{m}$  thick) were created by pressing 100 mg of powder, and pellets ranging from 3.5–4.8 mm thick were created by pressing 2 g of powder. All pellets were then reduced in 5%  $\text{H}_2$  (bal. Ar) by heating to 400  $^\circ\text{C}$  using a 5  $^\circ\text{C min}^{-1}$  ramp rate and holding for 3 hr to ensure the complete reduction of the samples and to minimize cracking. A

wrought Ni 200 (i.e., commercially pure) sample was cut from a rod, turned to comparable dimensions, and heated alongside the NiO samples for comparison in mechanical testing.

## 2.2 Characterization

Scanning electron microscopy (SEM) and scanning transmission electron microscopy (STEM) were performed with a JEOL IT-800 microscope operating at 1-5 kV (SEM) and 30 kV (STEM). Electron backscatter diffraction (EBSD) was performed with an Oxford Instruments Symmetry S2 detector and grain size analysis was performed in AZtecCrystal software. Focused ion beam (FIB) cross-sectioning was performed using an FEI Nova Nano Lab 600 dual beam microscope, and ion channeling contrast (ICC) images were generated at 30 kV. Broad beam ion milling (BBIM) was performed with a JEOL IB-19530CP. Particle size measurement was performed using a Malvern Mastersizer 3000, and particles were sonicated in isopropyl alcohol before measurement. Compressed pellets were subjected to quasi-static compression using an Instron 5982 electromechanical load frame with crosshead displacement speed of 0.5 mm/s (strain rate of  $\sim 2 \times 10^{-3} \text{ s}^{-1}$ ) to the load cell maximum of 100 kN. Hardened and polished compression surfaces were treated with a thin layer of graphite to reduce radial constraint.

## 3 Results and Discussion

As shown in Figure 1A, the Ni90NiO sample possesses a lower reduction onset temperature than AR-NiO or M-NiO. Jeangros et al. [42] studied the reduction of NiO nanoparticles by hydrogen using *in situ* environmental TEM (ETEM). They found that Ni domains nucleate on the NiO particles and accelerate the reaction and that no reduction occurs below 250 °C. This is consistent with the results for pure NiO presented here, but the onset temperature is lowered from  $\sim 260$  °C (as-received NiO) to  $\sim 180$  °C (Ni90NiO) because of the pre-existing metal-oxide interfaces [43]. When the as-received, pure Ni powder was reduced, the amount of moisture evolved was quite low, as the contribution is from a limited presence of native oxide (i.e., stored under Ar) on relatively large particles (10s of  $\mu\text{m}$ ), but the onset temperature is consistent with its role in accelerating reduction in Ni90NiO (see Figure 1A inset). This indicates that this process can be exceptionally environmentally friendly, with low temperatures and no chemical burden. In fact, the only byproduct of the process is water vapor. Furthermore, this process eliminates alloy residues, since no alloying addition is needed.

SEM imaging of a FIB cross-section of an as-milled Ni90NiO particle, as shown in Figure 1B and Figure 1C, reveals pre-existing porosity before reduction. Figure 1D reveals that the surface of a microscale particle appears as an agglomerate of nanoscale particles, and STEM imaging in Figure 1E and Figure 1F confirms this is the case. Because of the high NiO content, the Ni simply serves to bind the NiO particles together into larger agglomerates. The median particle diameter was measured to be 11.0  $\mu\text{m}$ , with a volume mean diameter of 4.97  $\mu\text{m}$ , and a span of 5.792. The 10<sup>th</sup> percentile size was 2.03  $\mu\text{m}$  and the 90<sup>th</sup> percentile size was 65.7  $\mu\text{m}$ . This emphasizes that the vast majority of the material is not in the form of isolated nanoparticles, the MMC particles vary widely in size, and they are structurally sound enough to endure the sonication process preceding analysis without disintegrating to discrete nanoparticles.

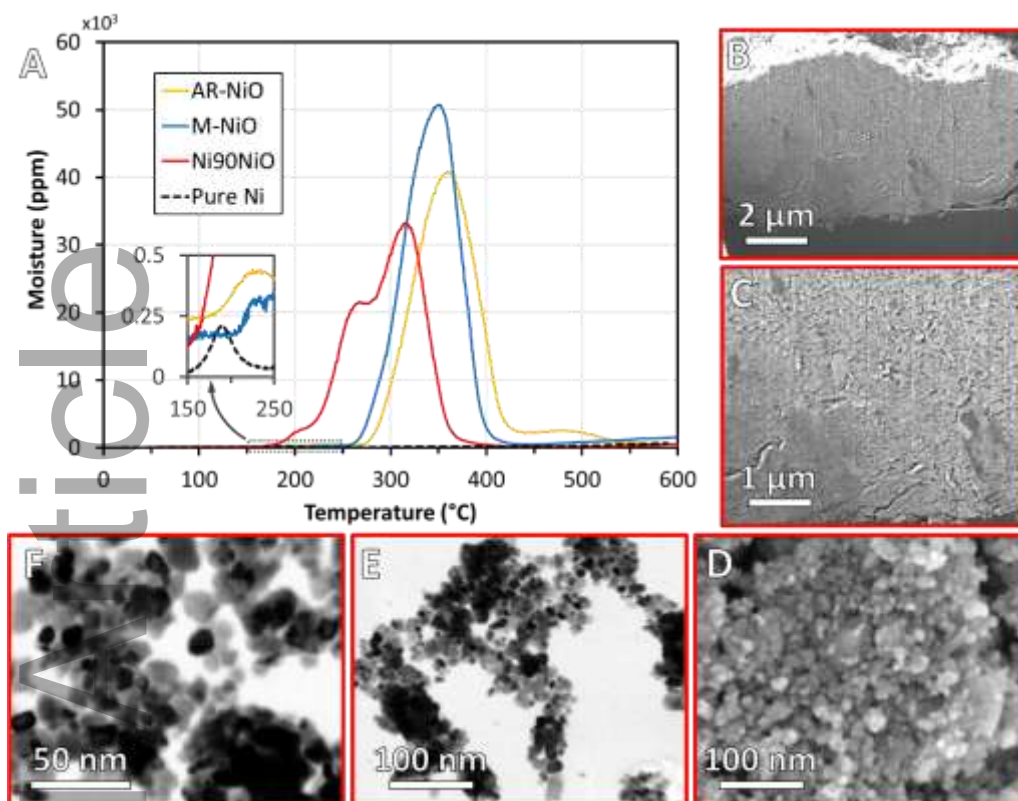


Figure 1 – (A) Reduction profiles during heating at  $5^{\circ}\text{C min}^{-1}$  to a maximum temperature of 600  $^{\circ}\text{C}$  for as-received NiO (AR-NiO), NiO milled for 1 hr (M-NiO), Ni 90 mol% NiO milled for 1 hr (Ni90NiO), and as-received, pure Ni powder. The as-milled structure of Ni90NiO was examined by (B, C) FIB sectioning and ICC imaging, (D) SEM of powder surface, and (E, F) STEM of loose powder.

When subjected to isothermal reduction (Figure 2A), the MMC particles convert to nanoporous particles at temperatures as low as 200  $^{\circ}\text{C}$  (Figure 2B), with similar results but shorter reaction times at 300  $^{\circ}\text{C}$  (Figure 2C) and 400  $^{\circ}\text{C}$  (Figure 2D). Because the 400  $^{\circ}\text{C}$  reduction quickly resulted in nanoscale porosity, it was chosen for further investigation. This included broad beam ion milling (BBIM), as shown in Figure 2E, and additional surface characterization (Figure 2F and Figure 2G). This pore formation process can be more rapid than chemical etching of similar sample sizes, as the reduction process is quick and the powder is usable as soon as it is reduced (no additional rinsing and drying steps).

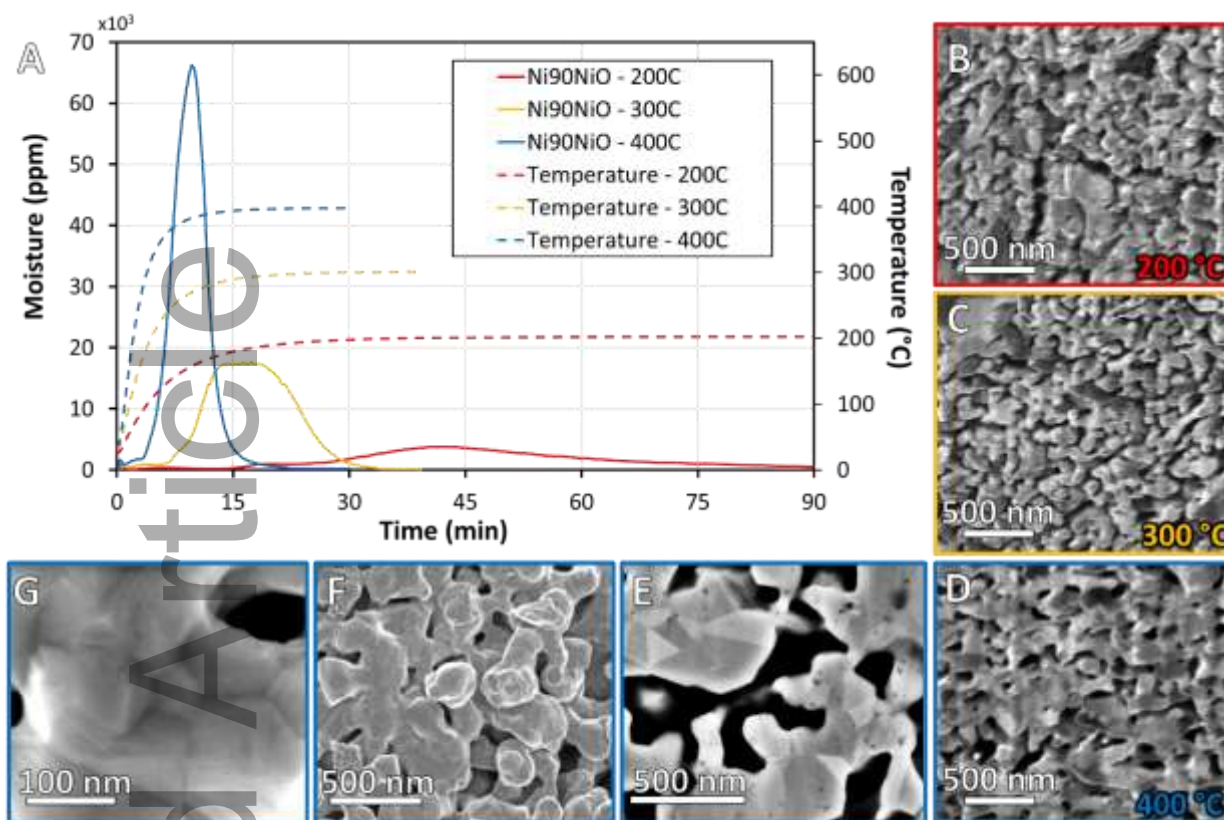


Figure 2 – (A) Reduction profiles of Ni90NiO and corresponding FIB ICC images after reduction at (B) 200 °C, (C) 300 °C, and (D) 400 °C. (E) BBIM section, and (F, G) surface images of Ni90NiO after reduction at 400 °C.

Ion channeling contrast (ICC) in Figure 2C-D and secondary electron grain contrast and surface faceting in Figure 2E-G suggest a nanoscale grain size in addition to the nanoporous character. To confirm this, BBIM was followed by EBSD analysis (see Figure 3). The cross-section is shown in Figure 3A with the corresponding orientation map in Figure 3B, which reveals a randomized grain orientation. The grain size distribution by number and volume average is shown in Figure 3C. Approximately 80% of the grains are below 200 nm by number, with approximately 40% below 200 nm by volume. The retention of this fine grain size after annealing at 400 °C is attributed to the combined stabilizing effects of the nanoscale oxide particles [44] and the porosity that forms after they are reduced. The formation of a nanocrystalline nanoporous structure may improve strength by contributing beyond the ligament scaling effect [45], and the already impressive radiation damage tolerance of np metals can be further improved by the additional defect sinks provided by grain boundaries [46].

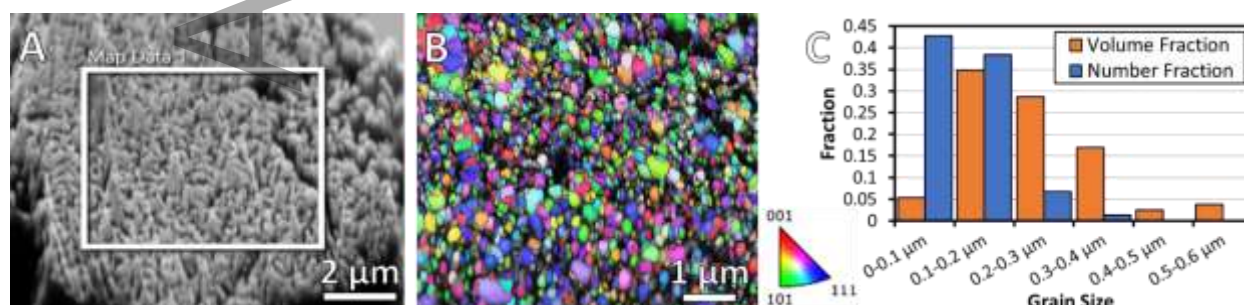


Figure 3 – (A) BBIM section of Ni90NiO reduced at 400 °C with (B) corresponding EBSD results, and (C) grain size distribution.

Manukyan, et al. [43] have provided a thorough account of NiO reduction in H<sub>2</sub> and the formation of porosity in micron NiO grains over a large range of temperatures. Our results are consistent with theirs in that AR-NiO and M-NiO will both produce nanoporous structures. Therefore, the formation of an MMC in Ni90NiO is not necessary for pore development, but it has other utility in processing. Challenges with creating useful devices from np metals often include scaling the process throughput or physical device dimensions. The application of powder precursors provides opportunity to use powder metallurgy (PM) methods, which are highly adaptable for part complexity and scale [47]. Dealloying has been previously applied to loose powders, with examples including commercial brass powders resulting in Cu particles with micron pores [30] as well as in mechanically alloyed Ag-Zn powders to create np Ag [48], although these reports do not include any bulk components comprised of these powders.

To investigate the production of bulk components and their properties disks and pellets were formed (see Figure 4). These two conformations are of interest for device fabrication, such as electrodes or catalysis, and for bulk applications such as actuation [49], respectively. It is evident in Figure 4A that these powders can be readily produced in thick sections, with the as-pressed pellets having a thickness ranging from 3.5-4.8 mm and a diameter of 12 mm. The AR-NiO had the lowest as-pressed relative density of 54% with the M-NiO and Ni90NiO each having densities of 73% (relative to NiO and the weighted average of 90% NiO and 10% Ni, respectively). The final relative densities of the pressed and reduced samples were 40%, 48%, and 53% for the AR-NiO, M-NiO, and Ni90NiO, respectively (relative to pure Ni). The AR-NiO was the only sample type to exhibit extensive radial cracking, with all exhibiting some circumferential cracking. Figures 4C-E show the as-reduced surfaces of the samples, with a decreasing size and proportion of porosity appearing commensurate with the final density. The as-pressed samples were not fragile, and could be readily handled without particular caution, even when made relatively thin (Figure 4F). The general applicability to PM processing may allow a diverse range of device fabrication geometries based on well-established protocol, making this method more commercially ready than most.

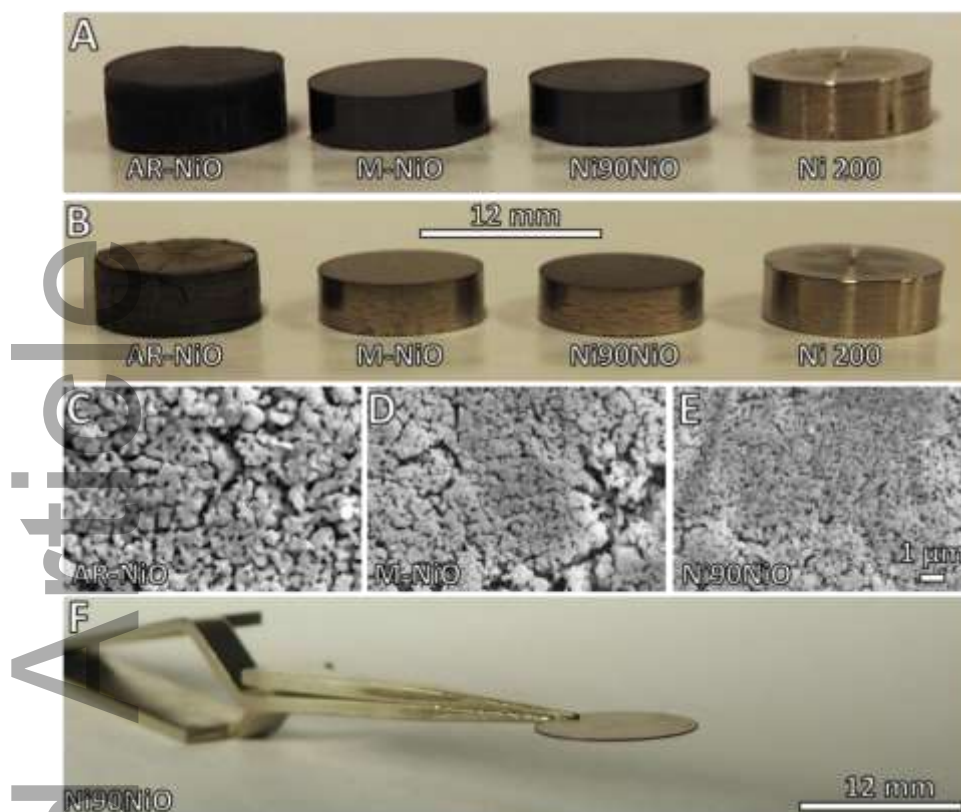


Figure 4 – (A) Bulk samples produced by uniaxial pressing of as-milled samples and wrought Ni (Ni 200) as-received, (B) the same samples after being reduced, SEM images of the top surface of (C) AR-NiO, (D) M-NiO, and (E) Ni90NiO after pressing and reducing, and (F) disc of Ni90NiO made by the same processes. All reductions performed at 400 °C in 5% H<sub>2</sub>.

In order to characterize the mechanical performance of these samples, they were subjected to uniaxial compression testing, and the resulting specific engineering stress vs engineering strain is shown in Figure 5A. The post-test samples for reduced and as-pressed compacts are shown in Figure 5B-E and Figure 5F-H, respectively. In both the as-pressed and the reduced conditions, the Ni90NiO shows slightly greater strength than the M-NiO, with the AR-NiO being substantially weaker, and the only sample to completely disintegrate during testing. This emphasizes the importance of the milling process to break up nanoparticle agglomerates, thereby resulting in higher as-pressed density and strength. The importance of the Ni addition as a binder and to promote the reduction and sintering process is also demonstrated. The reduced samples display extensive plasticity despite some fracturing along their circumferences, and their specific strength and mechanical response was nearly identical to that of wrought Ni. This is significant, because producing mechanically robust np Ni is a challenge [50].

The remaining “core” of intact material after compression testing was still mechanically stable and easily handled without breaking. It is important to emphasize these samples were never heated above 400 °C (0.39 T<sub>M</sub>, Ni), which is lower than recommended for making even *porous* metals by PM [51] and which limits mechanical integrity in general. Higher temperatures may improve the mechanical response but associated coarsening would need to be considered as well [52]. As noted by Taylor et al. in their work on 3D printing of Ni from NiO inks [53], the reduction process provides enhanced diffusion that promotes sintering. Enhanced diffusion is an important factor here for creating structurally sound samples at such low processing temperatures. Unlike most PM processes, the reducing/sintering process results in lower relative density rather than increasing density. This is because bulk diffusive transport, which drives densification, is minimal, even if surface diffusion can promote particle bonding [54].

This article is protected by copyright. All rights reserved

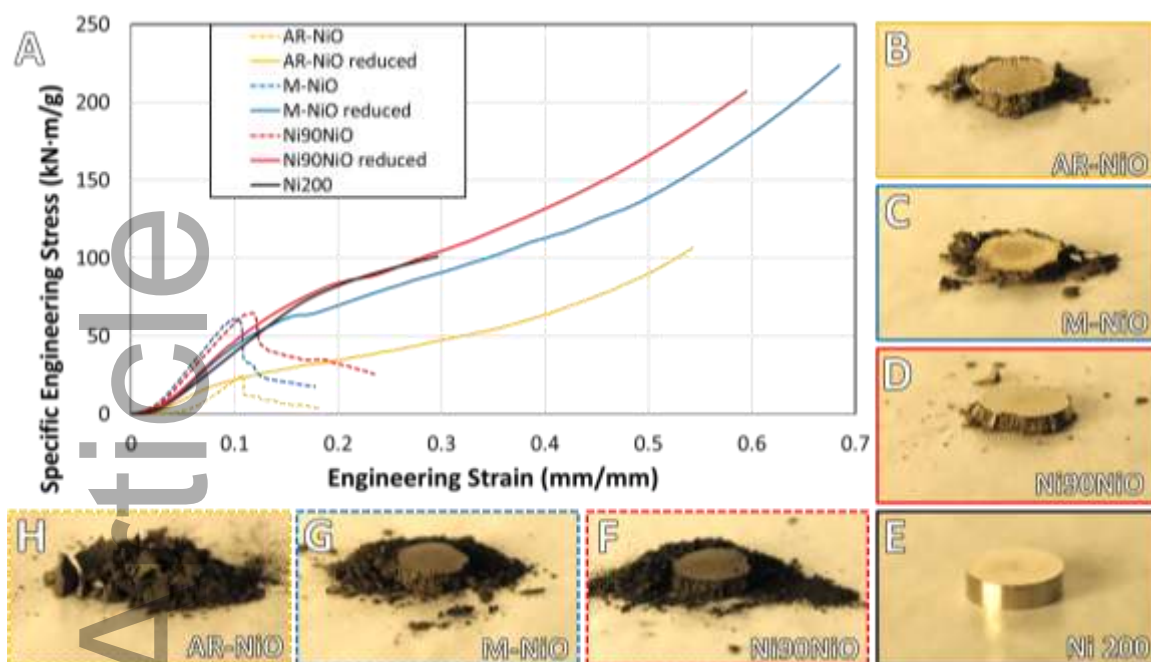


Figure 5 – (A) Stress-strain compression results, the resulting deformation of reduced samples (B) AR-NiO, (C) M-NiO, (D) Ni90NiO, (E) Ni 200, and the compression results of as-pressed samples of (F) Ni90NiO, (G) M-NiO, and (H) AR-NiO.

Porous Ni has many potential applications, such as energy storage [55-57], fuel cells [58, 59], and catalysis [60], which account for its rapid rise in publication frequency [61]. Though not prevalent in dealloying literature, np Ni has been produced by dealloying Ni-Mn [56, 62], Ni-Mn-Cu [55], or classic Ni-Al alloys (e.g., [63]), first developed and patented by Murray Raney in 1927 [64]. While np Ni precursors may not require some of the harshest chemistries, such as hydrofluoric or nitric acids, the Ni-Mn precursors noted above use ammonium sulfide and the Raney process uses sodium hydroxide. Both chemicals require significant precautions for personnel safety and environmental release. This work establishes a viable method to make np Ni at scale using basic equipment and without any chemical burden. The powder-based nature of the precursor lends itself to diverse applications, including traditional powder metallurgy and additive manufacturing techniques. The primary concern for safety and environment is the fine NiO powder used to develop the precursor mixture used here. Is it reasonable to expect that micron NiO powder can be used instead of nanoscale powder and then refined during the milling process. The primary advantage of oxide reduction for pore formation is that there is no waste product, as the NiO is converted to Ni in the final product, unlike liquid etchants and the metal ions they leach from the alloy, regardless of the initial chemistry. The minimal energy of the process is also notable, as it does not require high temperature for melt processing, as is often used for precursor formation or liquid metal dealloying, or even the more modest energy required in high-vacuum vaporization of a sacrificial element such as zinc.

The main limitation to this technique is the reduction step, such that metals with high affinity for oxygen, appearing low on an Ellingham diagram [65], will not be readily made this way. This provides a restricted selection comparable to traditional dealloying, where the process is typically applied to produce relatively noble metals, though Ni is often not among them. Developments in liquid and vapor-phase dealloying have extended the range of np metals and alloys but with an attendant increase in complexity. Oxide reduction also allows for the production of alloys (e.g., [40, 41]), as long as the alloying elements are able to be reduced at temperatures where associated microstructural coarsening is not prohibitive.

This article is protected by copyright. All rights reserved

## 4 Conclusions

The production of nanoporous metals and alloys is often accomplished through dealloying. The methods to perform it are becoming increasingly sophisticated and diverse, but there are still central challenges. This work addresses four distinct and important shortcomings of current methods: (1) simple, scalable production of precursor materials, (2) no hazardous chemicals, byproducts, or residues, (3) bulk geometries readily made, and (4) mechanically robust structure results. All four of these are achieved using the vapor phase reduction of oxide particles processed through ball milling. This is demonstrated in the Ni-NiO system, where nanoporous Ni is produced by the hydrogen reduction of NiO. When 10 mol% Ni is added to the NiO, the reduction process can be performed at temperatures as low as 200 °C, though the reaction is greatly accelerated at 400 °C. The Ni-NiO composite also displays greater mechanical stability after pressing into bulk geometries and after subsequent reduction. Samples were made by compaction in a 12 mm diameter die, in which samples of varying thickness could be produced and handled reliably. When normalized for density, the Ni-NiO precursor performed nearly identically to wrought Ni in compression testing, showing only modest cracking along the perimeter of the 12 mm diameter pellet, even after 50% strain. The low-cost, simple processing strategies along with bulk part formation and mechanical performance are unique to this work and may provide needed advancements for the commercialization of nanoporous metals.

## Declaration of Competing Interest

The authors declare that they have no known competing financial interests or personal relationships that could have appeared to influence the work reported in this paper.

## Acknowledgements

This work was made possible by the characterization support of Craig Theberg of JEOL USA, Inc (HR-SEM, BBIM, and STEM), Sam Pennington of Oxford Instruments America, Inc. (EBSD), Chad Hornbuckle of Army Research Lab, APG, MD (FIB sections and ICC), and Materials Characterization Laboratory at Pennsylvania State University (particle size analysis). Financial support was provided by the National Science Foundation [CAREER Award # 2035473].

## References

1. Newman, R., S. Corcoran, J. Erlebacher, M. Aziz, K. Sieradzki, *Alloy corrosion*. MRS Bull. **1999**, 24, 24.
2. McCue, I., E. Benn, B. Gaskey, J. Erlebacher, *Dealloying and dealloyed materials*. Ann. Rev. Mater. Res. **2016**, 46, 263.
3. Erlebacher, J., K. Sieradzki, *Pattern formation during dealloying*. Scripta Mater. **2003**, 49, 991.
4. Erlebacher, J., M.J. Aziz, A. Karma, N. Dimitrov, K. Sieradzki, *Evolution of nanoporosity in dealloying*. Nature **2001**, 410, 450.
5. Detsi, E., M. Van De Schootbrugge, S. Punzhin, P. Onck, J. De Hosson, *On tuning the morphology of nanoporous gold*. Scripta Mater. **2011**, 64, 319.
6. Sun, L., C.-L. Chien, P.C. Searson, *Fabrication of nanoporous nickel by electrochemical dealloying*. Chem. Mater. **2004**, 16, 3125.

7. Wang, X., J. Sun, C. Zhang, T. Kou, Z. Zhang, *On the microstructure, chemical composition, and porosity evolution of nanoporous alloy through successive dealloying of ternary Al–Pd–Au precursor*. J. Phys. Chem. C **2012**, 116, 13271.
8. Zou, L., M. Ge, C. Zhao, Q. Meng, H. Wang, X. Liu, C.-H. Lin, X. Xiao, W.-K. Lee, Q. Shen, *Designing Multiscale Porous Metal by Simple Dealloying with 3D Morphological Evolution Mechanism Revealed via X-ray Nano-tomography*. ACS Appl. Mater. Interfaces **2019**, 12, 2793.
9. Dan, Z., F. Qin, Y. Sugawara, I. Muto, A. Makino, N. Hara, *Nickel-stabilized nanoporous copper fabricated from ternary TiCuNi amorphous alloys*. Mater. Lett. **2013**, 94, 128.
10. Zeng, Y., B. Gaskey, E. Benn, I. McCue, G. Greenidge, K. Livi, X. Zhang, J. Jiang, J. Elebacher, *Electrochemical dealloying with simultaneous phase separation*. Acta Mater. **2019**, 171, 8.
11. Yu, J., Y. Ding, C. Xu, A. Inoue, T. Sakurai, M. Chen, *Nanoporous Metals by Dealloying Multicomponent Metallic Glasses*. Chem. Mater. **2008**, 20, 4548.
12. Zhang, H., J. Fornell, Y. Feng, I. Golvano, M.D. Baró, E. Pellicer, J. Sort, *Inducing surface nanoporosity on Fe-based metallic glass matrix composites by selective dealloying*. Mater Charact **2019**, 153, 46.
13. Wang, X., R. Li, Z. Li, R. Xiao, X.-B. Chen, T. Zhang, *Design and preparation of nanoporous Ag–Cu alloys by dealloying Mg–(Ag, Cu)–Y metallic glasses for antibacterial applications*. J. Mater. Chem. B **2019**, 7, 4169.
14. Snyder, J., P. Asanithi, A.B. Dalton, J. Erlebacher, *Stabilized nanoporous metals by dealloying ternary alloy precursors*. Adv. Mater. **2008**, 20, 4883.
15. Joo, S.H., J.W. Bae, W.Y. Park, Y. Shimada, T. Wada, H.S. Kim, A. Takeuchi, T.J. Konno, H. Kato, I.V. Okulov, *Beating thermal coarsening in nanoporous materials via high-entropy design*. Adv. Mater. **2020**, 32, 1906160.
16. McCue, I., B. Gaskey, P.-A. Geslin, A. Karma, J. Erlebacher, *Kinetics and morphological evolution of liquid metal dealloying*. Acta Mater. **2016**, 115, 10.
17. Geslin, P.-A., I. McCue, B. Gaskey, J. Erlebacher, A. Karma, *Topology-generating interfacial pattern formation during liquid metal dealloying*. Nat. Commun. **2015**, 6, 8887.
18. Wada, T., K. Yubuta, A. Inoue, H. Kato, *Dealloying by metallic melt*. Mater. Lett. **2011**, 65, 1076.
19. Zhao, C., T. Wada, V. De Andrade, G.J. Williams, J. Gelb, L. Li, J. Thieme, H. Kato, Y.-c.K. Chen-Wiegart, *Three-Dimensional Morphological and Chemical Evolution of Nanoporous Stainless Steel by Liquid Metal Dealloying*. ACS Appl. Mater. Interfaces **2017**, 9, 34172.
20. Gaskey, B., I. McCue, A. Chuang, J. Erlebacher, *Self-assembled porous metal-intermetallic nanocomposites via liquid metal dealloying*. Acta Mater. **2019**, 164, 293.
21. Kim, J.W., T. Wada, S.G. Kim, H. Kato, *Enlarging the surface area of an electrolytic capacitor of porous niobium by MgCe eutectic liquid dealloying*. Scripta Mater. **2016**, 122, 68.
22. Wada, T., P.-A. Geslin, H. Kato, *Preparation of hierarchical porous metals by two-step liquid metal dealloying*. Scripta Mater. **2018**, 142, 101.
23. Shao, J.-C., H.-J. Jin, *From liquid metal dealloying to liquid metal expulsion*. J. Mater. Sci. **2020**, 55, 8337.
24. McCue, I., M.J. Demkowicz, *Alloy Design Criteria for Solid Metal Dealloying of Thin Films*. JOM **2017**, 69, 2199.
25. Zhao, C., K. Kisslinger, X. Huang, M. Lu, F. Camino, C.-H. Lin, H. Yan, E. Nazaretski, Y. Chu, B. Ravel, *Bi-continuous pattern formation in thin films via solid-state interfacial dealloying studied by multimodal characterization*. Mater. Horiz. **2019**, 6, 1991.
26. Lu, Z., C. Li, J. Han, F. Zhang, P. Liu, H. Wang, Z. Wang, C. Cheng, L. Chen, A. Hirata, *Three-dimensional bicontinuous nanoporous materials by vapor phase dealloying*. Nat. Commun. **2018**, 9, 1.
27. Barroo, C., M.M. Montemore, N. Janvelyan, B. Zugic, A.J. Akey, A.P. Magyar, J. Ye, E. Kaxiras, J. Biener, D.C. Bell, *Macroscopic 3D nanoporosity formation by dry oxidation of AgAu alloys*. J. Phys. Chem. C **2017**, 121, 5115.
28. Murzin, S.P., *Exposure to laser radiation for creation of metal materials nanoporous structures*. Opt. Laser Technol. **2013**, 48, 509.

29. Murzin, S.P., *Formation of nanoporous structures in metallic materials by pulse-periodic laser treatment*. Opt. Laser Technol. **2015**, 72, 48.
30. Sun, Y., Y. Ren, *New preparation method of porous copper powder through vacuum dealloying*. Vacuum **2015**, 122, 215.
31. Sun, Y., Y. Ren, K. Yang, *New preparation method of micron porous copper through physical vacuum dealloying of Cu–Zn alloys*. Mater. Lett. **2016**, 165, 1.
32. Wang, C., Q. Chen, *Reduction-induced decomposition: spontaneous formation of monolithic nanoporous metals of tunable structural hierarchy and porosity*. Chem. Mater. **2018**, 30, 3894.
33. Zhang, A., J. Wang, P. Schützendübe, H. Liang, Y. Huang, Z. Wang, *Beyond dealloying: development of nanoporous gold via metal-induced crystallization and its electrochemical properties*. Nanotechnology **2019**, 30, 375601.
34. Shin, H.-C., J. Dong, M. Liu, *Nanoporous Structures Prepared by an Electrochemical Deposition Process*. Adv. Mater. **2003**, 15, 1610.
35. Plowman, B.J., L.A. Jones, S.K. Bhargava, *Building with bubbles: the formation of high surface area honeycomb-like films via hydrogen bubble templated electrodeposition*. Chem. Commun. **2015**, 51, 4331.
36. Tappan, B.C., S.A. Steiner III, E.P. Luther, *Nanoporous metal foams*. Angew. Chem., Int. Ed. **2010**, 49, 4544.
37. Ron, R., E. Haleva, A. Salomon, *Nanoporous metallic networks: fabrication, optical properties, and applications*. Adv. Mater. **2018**, 30, 1706755.
38. Petkovich, N.D., A. Stein, *Controlling macro-and mesostructures with hierarchical porosity through combined hard and soft templating*. Chem. Soc. Rev. **2013**, 42, 3721.
39. Atwater, M.A., K.A. Darling, M.A. Tschopp, *Towards Reaching the Theoretical Limit of Porosity in Solid State Metal Foams: Intraparticle Expansion as a Primary and Additive Means to Create Porosity*. Adv. Eng. Mater. **2014**, 16, 190.
40. Atwater, M.A., T.L. Luckenbaugh, B.C. Hornbuckle, K.A. Darling, *Solid State Foaming of Nickel, Monel, and Copper by the Reduction and Expansion of NiO and CuO Dispersions*. Adv. Eng. Mater. **2018**, 20, 1800302.
41. Atwater, M.A., S.J. Fudger, C.B. Nelson, B.C. Hornbuckle, S.J. Knauss, S.A. Brennan, K.A. Darling, *Multi-stage pore development in Ag foams by the reduction of Ag<sub>2</sub>O and CuO mixtures*. Mater. Des. **2020**, 186, 108273.
42. Jeangros, Q., T.W. Hansen, J.B. Wagner, C.D. Damsgaard, R.E. Dunin-Borkowski, C. Hébert, A. Hessler-Wyser, *Reduction of nickel oxide particles by hydrogen studied in an environmental TEM*. J. Mater. Sci. **2013**, 48, 2893.
43. Manukyan, K.V., A.G. Avetisyan, C.E. Shuck, H.A. Chatilyan, S. Rouvimov, S.L. Kharatyan, A.S. Mukasyan, *Nickel oxide reduction by hydrogen: kinetics and structural transformations*. J. Phys. Chem. C **2015**, 119, 16131.
44. Nes, E., N. Ryum, O. Hunderi, *On the Zener drag*. Acta Metall. **1985**, 33, 11.
45. Zhao, M., I. Issa, M.J. Pfeifenberger, M. Wurmschuber, D. Kiener, *Tailoring ultra-strong nanocrystalline tungsten nanofoams by reverse phase dissolution*. Acta Mater. **2020**, 182, 215.
46. Li, J., C. Fan, J. Ding, S. Xue, Y. Chen, Q. Li, H. Wang, X. Zhang, *In situ heavy ion irradiation studies of nanopore shrinkage and enhanced radiation tolerance of nanoporous Au*. Sci. Rep. **2017**, 7, 39484.
47. Eisen, W.B., *Powder metal technologies and applications*, in ASM Handbook, B.L. Ferguson, et al., Editors. **1998**, ASM International: Novelty, OH
48. Bhushan, B., B. Murty, K. Mondal, *A two-step method for synthesis of micron sized nanoporous silver powder and ZnO nanoparticles*. Adv. Powder Technol. **2017**, 28, 2532.
49. Jin, H.J., J. Weissmüller, *Bulk nanoporous metal for actuation*. Adv. Eng. Mater. **2010**, 12, 714.
50. Lühns, L., J. Weissmüller, *Nanoporous copper-nickel-macroscopic bodies of a strong and deformable nanoporous base metal by dealloying*. Scripta Mater. **2018**, 155, 119.
51. Liu, P., G. Chen, *Making porous metals*, in Porous Materials. **2014**. 21.

52. Chen-Wiegart, Y.-c.K., S. Wang, Y.S. Chu, W. Liu, I. McNulty, P.W. Voorhees, D.C. Dunand, *Structural evolution of nanoporous gold during thermal coarsening*. Acta Mater. **2012**, 60, 4972.
53. Taylor, S.L., A.E. Jakus, R.N. Shah, D.C. Dunand, *Iron and Nickel Cellular Structures by Sintering of 3D-Printed Oxide or Metallic Particle Inks*. Adv. Eng. Mater. **2017**, 19, 1600365.
54. German, R.M., *Sintering Trajectories: Description on How Density, Surface Area, and Grain Size Change*. JOM **2016**, 68, 878.
55. Qiu, H.-J., Y. Ito, M. Chen, *Hierarchical nanoporous nickel alloy as three-dimensional electrodes for high-efficiency energy storage*. Scripta Mater. **2014**, 89, 69.
56. Qiu, H.-J., J. Kang, P. Liu, A. Hirata, T. Fujita, M. Chen, *Fabrication of large-scale nanoporous nickel with a tunable pore size for energy storage*. J. Power Sources **2014**, 247, 896.
57. Sang, Q., S. Hao, J. Han, Y. Ding, *Dealloyed nanoporous materials for electrochemical energy conversion and storage*. EnergyChem **2022**, 100069.
58. Park, H., C. Ahn, H. Jo, M. Choi, D.S. Kim, D.K. Kim, S. Jeon, H. Choe, *Large-area metal foams with highly ordered sub-micrometer-scale pores for potential applications in energy areas*. Mater. Lett. **2014**, 129, 174.
59. Jo, H., M.J. Kim, H. Choi, Y.-E. Sung, H. Choe, D.C. Dunand, *Morphological study of directionally freeze-cast nickel foams*. Metall. Mater. Trans. E **2016**, 3, 46.
60. Atwater, M.A., L.N. Guevara, S.J. Knauss, *Multifunctional Porous Catalyst Produced by Mechanical Alloying*. Mater. Res. Lett. **2019**, 7, 131.
61. Atwater, M.A., L.N. Guevara, K.A. Darling, M.A. Tschopp, *Solid State Porous Metal Production: A Review of the Capabilities, Characteristics, and Challenges*. Adv. Eng. Mater. **2018**, 20, 1700766.
62. Dan, Z., F. Qin, Y. Sugawara, I. Muto, N. Hara, *Bimodal nanoporous nickel prepared by dealloying Ni<sub>38</sub>Mn<sub>62</sub> alloys*. Intermetallics **2012**, 31, 157.
63. Ren, X., Y. Zhai, Q. Zhou, J. Yan, S. Liu, *Fabrication of nanoporous Ni and NiO via a dealloying strategy for water oxidation catalysis*. J. Energy Chem. **2020**, 125.
64. Murray, R., *Method of producing finely-divided nickel*. **1927**, US1628190A.
65. Gaskell, D.R., *Introduction to the Thermodynamics of Materials*. 4th ed. **2003**, New York, NY: Taylor and Francis.

## Graphical TOC

A method for producing nanoporous Ni is described that is low cost and scalable, and the only processing byproduct is water vapor. A metal-matrix composite of Ni and NiO is reduced under dilute hydrogen to create pure Ni with nanocrystalline structure and nanoscale porosity. The technique is demonstrated in loose powder as well as in thin and bulk compacts.

